

We consider that, in (1)–(3), all variables are dimensionless. If governing equation (1) was deduced from a physical problem, dimensionless parameters should appear in it. However, for simplicity, we assume that those parameters are equal to unity. This may be justified by the fact that the present study is mainly focused on the development of a numerical method rather than on a particular physical problem.

Since (1) is of parabolic nature, one might think that, according to many classical examples [6], the spreading rate of the slick should be infinite, i.e., the slick should cover the whole accessible domain within an infinitely short time. It may be hypothesized that the spreading rate remains finite because κ is zero on the edge—where $h = 0$.

One is thus faced with a nonlinear advection-diffusion problem that must be treated in a variable domain, the size of which modifies according to the dynamics of the solution itself.

The numerical solution of (1) should be conducted carefully. Suppose that a simple finite volume technique [7] is used and that the size of the grid cells remains unchanged as the time passes. Consider two adjacent grid boxes: in one of them $h > 0$, while $h = 0$ in the other. If the advection is negligible, the diffusion flux is likely to be such that, within one single time step, the edge of the slick will reach the center of the grid box where the thickness was initially zero. Thus, if Δx and Δt denote the space and time increments of the numerical method, the boundary of the slick will expand at a velocity of order $\Delta x/\Delta t$, which is completely wrong! Clearly, introducing significant advection processes into the model would not render the numerical solution more reliable.

It is doubtless that any reasonably accurate numerical solution of (1) must rely, in a relevant manner, on an estimation of the velocity of the slick's edge.

If a dynamically adaptive grid fitted to the slick's boundary is implemented, determining the velocity of the edge is evidently of crucial importance [8]. And, even if a fixed grid is used, it is clear that the knowledge of the edge's velocity will help improve the accuracy of the numerical solution.

In the present paper, one first derives an asymptotic expression of the velocity of the edge of the slick, which can be easily introduced into a numerical method. Next, preliminary tests of the validity of this approximate expression are conducted for an axisymmetric problem where an exact analytical solution exists. Finally, the relevance of the tests is discussed and some peculiarities of the numerical method utilized are highlighted.

2. AN ASYMPTOTIC EXPRESSION OF THE EDGE'S VELOCITY

We consider the solution of (1) in a two-dimensional unbounded domain. Moreover, we assume that the initial area of the slick—at $t = 0$ —is finite so that there exists a curve, the slick's edge, separating the region where $h = 0$ from that where $h > 0$. Since we want to describe the motion of the edge of the slick, it is appropriate to introduce a local coordinate system (η, ξ) having its origin at the edge and defined so that $h > 0$ where $\eta < 0$ (Figure 1). Unit vectors \mathbf{e}_η and \mathbf{e}_ξ , associated with the local coordinates η and ξ , are, respectively, normal and tangential to the edge. The advection velocity, \mathbf{v} , and the velocity of the edge, \mathbf{u} , may be written as

$$(\mathbf{v}, \mathbf{u}) = (v_\eta, u_\eta)\mathbf{e}_\eta + (v_\xi, u_\xi)\mathbf{e}_\xi. \quad (4)$$

In the local coordinate system, which moves with the edge of the slick, the time derivative transforms to

$$\frac{\partial}{\partial t} = \frac{\partial}{\partial \tau} - u_\eta \frac{\partial}{\partial \eta} - u_\xi \frac{\partial}{\partial \xi}, \quad (5)$$

where τ represents the "time coordinate" associated with the moving reference framework. Of course, $\tau = t$.

One must bear in mind that we have not demonstrated that u_η and u_ξ must be finite. We have only made this hypothesis. Nevertheless, when seeking an asymptotic expression, it is always necessary to first introduce a set of credible assumptions. And, if the ensuing mathematical developments do not lead to absurd results, the assumptions put forward beforehand may then be deemed valid.

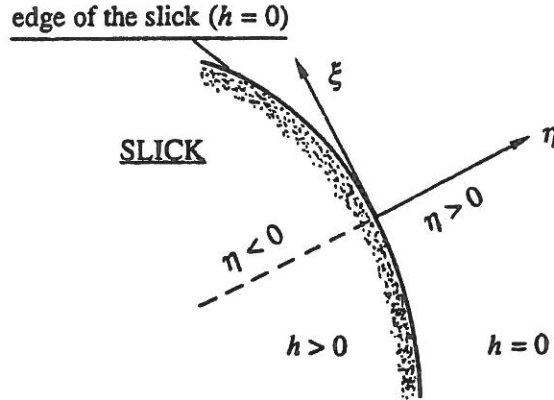


Figure 1. Illustration of the local coordinate system attached to the edge of the slick.

In accordance with this philosophy, one also assumes that the length scale along the η -axis is much smaller than that along the ξ -axis. Thus,

$$\frac{\partial}{\partial \eta} \gg \frac{\partial}{\partial \xi}. \quad (6)$$

It is also convenient to neglect the role of Q in the vicinity of the edge. This hypothesis cannot be justified in general, since the reasoning should depend on the specific parameterizations of the production/destruction terms. It is just for simplicity that this assumption is called on here.

Introducing all of the above definitions and assumptions into (1), an asymptotic form is obtained that is all the more valid as the edge of the slick is approached:

$$\frac{\partial h}{\partial \tau} - u_{\eta} \frac{\partial h}{\partial \eta} \sim - \frac{\partial}{\partial \eta} \left(v_{\eta} h - h^a \frac{\partial h}{\partial \eta} \right), \quad \eta \rightarrow 0. \quad (7)$$

In the vicinity of the edge, it is assumed that h admits a simple asymptotic expansion, namely

$$h \sim H(\tau)(-\eta)^b, \quad \eta \rightarrow 0, \quad (8)$$

with $\eta \leq 0$. Expression (8) implies that the second term in the left hand side of (7) is dominant relative to the first. Indeed, it is easily shown that

$$\frac{\left| \frac{\partial h}{\partial \tau} \right|}{\left| u_{\eta} \frac{\partial h}{\partial \eta} \right|} = \left| \frac{1}{b u_{\eta}} \frac{\partial H}{\partial \tau} \right| (-\eta) \rightarrow 0, \quad \eta \rightarrow 0. \quad (9)$$

It is conceivable that, in most cases, the following simplification holds true near the edge of the slick:

$$\frac{\partial(v_{\eta} h)}{\partial \eta} \sim v_{\eta} \frac{\partial h}{\partial \eta}. \quad (10)$$

In view of (9)–(10), (7) asymptotically reduces to

$$(v_{\eta} - u_{\eta}) \frac{\partial h}{\partial \eta} \sim \frac{\partial}{\partial \eta} \left(h^a \frac{\partial h}{\partial \eta} \right), \quad \eta \rightarrow 0, \quad (11)$$

meaning that, in the local coordinate system, the advective terms are approximately balanced by the diffusive ones.

Substituting (8) into (11), assuming that all terms have the same order of magnitude, one has

$$b = \frac{1}{a}. \quad (12)$$

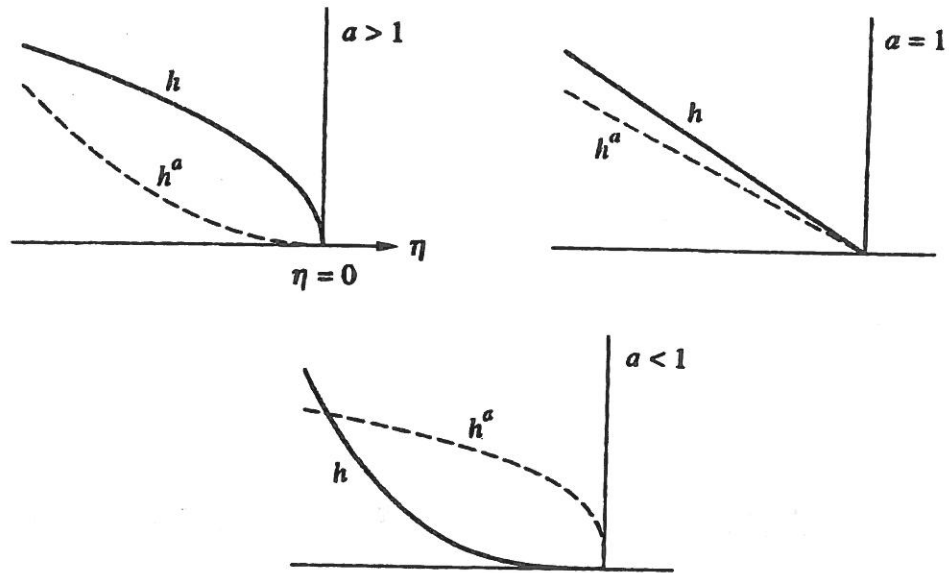


Figure 2. Profiles in the vicinity of the slick's edge of the thickness, h , and of the diffusion coefficient, h^a , for various values of exponent a .

Thus, as shown in Figure 2, $\frac{\partial h}{\partial \eta}$ at the edge is infinite, finite, or zero according to whether a is > 1 , $= 1$, or < 1 .

Combining (8), (11), and (12) yields

$$u_\eta = v_\eta + \frac{H^a}{a}, \quad (13)$$

which means that the edge moves under the joint effect of advection and diffusion, the latter being accounted for by velocity H^a/a .

In a finite difference or finite volume method, one may take advantage of (13) in a simple manner. If L denotes the distance to the edge of the first grid point where $h > 0$, then, according to (8) (Figure 3),

$$h_L \equiv h(\eta = -L) \sim L^{1/a} H. \quad (14)$$

By combining (13) and (14), an approximate expression of the velocity of the slick's edge is obtained:

$$u_\eta \sim v_\eta + \frac{(h_L)^a}{aL}, \quad L \rightarrow 0. \quad (15)$$

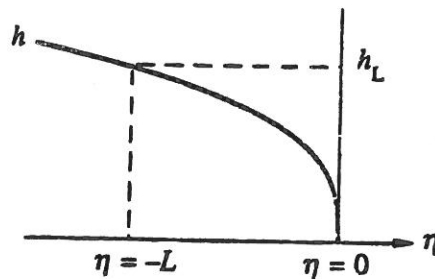


Figure 3. Illustration of the way to implement approximation (15) of the edge's velocity in a numerical method. Quantity L is the distance to the edge of the last grid point located inside the slick.

It is believed that asymptotic expressions (8) and (15) may be equally helpful when a finite element technique is chosen.

It was necessary to resort to many hypotheses to establish relations (8), (13), and (15). Whether or not these relations may be applied to any kind of slick is far from clear. Thus, it may be found useful to examine their relevance in a case where the exact solution of (1) is known.

3. AN EXACT SOLUTION

When Q is negligible and when the advection velocity exhibits negligible variations over the slick's area, one may study the spreading of the slick in a reference framework moving with the center of gravity of the slick. If it is further assumed that an axisymmetric spreading regime prevails, the evolution of the slick is governed by

$$\frac{\partial h}{\partial t} = \frac{1}{r} \frac{\partial}{\partial r} \left(r h^a \frac{\partial h}{\partial r} \right), \quad (16)$$

where r is a polar coordinate having its origin at the slick's center of gravity.

Equation (16) admits an exact solution [6]

$$h(t, r) = \frac{(a+1)\Omega}{\pi a R^2} \left[1 - \left(\frac{r}{R} \right)^2 \right]^{1/a}, \quad (17)$$

where R denotes the radius of the slick ($0 \leq r \leq R$), which grows according to

$$R(t) = \left[R_0^{2a+2} + \frac{4}{\pi^a} \left(\frac{a+1}{a} \right)^{a+1} \Omega^a t \right]^{1/(2a+2)}, \quad (18)$$

with $R(t=0) = R_0$. Since the production/destruction term Q is zero in (16), the volume of the slick,

$$\Omega = 2\pi \int_0^R h r dr, \quad (19)$$

remains constant as time increases. This is easily checked.

Near the edge of the slick, the local coordinate η is defined to be

$$\eta = r - R. \quad (20)$$

It is readily seen that (17) admits an asymptotic expansion of the form

$$h \sim \frac{2^{1/a}(a+1)\Omega}{\pi a R^{2+1/a}} (-\eta)^{1/a}, \quad \eta \rightarrow 0, \quad (21)$$

which is in agreement with (8), provided one sets

$$H = \frac{2^{1/a}(a+1)\Omega}{\pi a R^{2+1/a}}. \quad (22)$$

Since

$$R' \equiv \frac{dR}{dt} = \frac{2(a+1)^a \Omega^a}{\pi^a a^{a+1} R^{2a+1}}, \quad (23)$$

it is easily seen that the velocity of the edge of the slick, $u_\eta \equiv R'$, satisfies

$$R' = \frac{H^a}{a}, \quad (24)$$

which is in fact relation (13) adapted to the simple case examined in this section.

All this turns out to be reassuring as to the validity of the asymptotic analysis performed above. However, it must be kept in mind that the exact solution is so simple that it identically satisfies some of the assumptions underlying the asymptotic relations previously derived. As a matter of fact, only (8) and (9) are not verified *a priori* in our axisymmetric problem.

Further testing of the asymptotic results is obviously necessary. Accordingly, it will be shown that an accurate numerical technique can be built by using asymptotic expression (15).

4. NUMERICAL EXPERIMENTS

We are going to compare numerical solutions with the single exact solution we have. Thus, a numerical algorithm, which uses (15), will be built in order to provide the solution of axisymmetric equation (16).

To solve (16), it is desirable to work with a space discretization based on a moving grid fitted to the slick's edge. To do so, the following change of variable is called on:

$$(\tau, \theta) = \left(t, \frac{r}{R} \right), \quad (25)$$

with $\tau \geq 0$ and $0 \leq \theta \leq 1$. With these new variables, governing equation (16) transforms to

$$\frac{\partial}{\partial \tau} (R^2 \theta h) = \frac{\partial}{\partial \theta} \left(RR' \theta^2 h + \theta h^a \frac{\partial h}{\partial \theta} \right), \quad (26)$$

which is a conservative form that is well-suited to most numerical techniques.

For the solution of (26) to be equal to (17), the initial profile of the slick must be given by

$$h(\tau = 0, \theta) = \frac{(a+1)\Omega}{\pi a R_0^2} [1 - \theta^2]^{1/a}. \quad (27)$$

A linear transformation of time τ would permit re-scaling Ω and R_0 so that both of those quantities would become equal to unity. Thus, without any loss of generality, all numerical calculations may be carried out with

$$(\Omega, R_0) = (1, 1). \quad (28)$$

If $\Delta\tau$ and $\Delta\theta$, respectively, denote the time step and the space increment, $h_{n,k}$ is defined to be

$$h_{n,k} = h(\tau_n, \theta_k), \quad (29)$$

with $\tau_{n+1} = \tau_n + \Delta\tau_n$ ($n = 0, 1, 2, \dots$; $\tau_0 = 0$) and $\theta_k = (k - \frac{1}{2})\Delta\theta$ ($k = 1, 2, \dots, K$), where K represents the number of grid points ($\Delta\theta = \frac{1}{K}$).

Fully implicit time stepping proved to be slightly less accurate but much more stable than a Crank-Nicholson one. Taking advantage of the conservative nature of (26), the following finite volume discretization of (26) is derived:

$$\frac{R_{n+1}^2 \theta_k h_{n+1,k} - R_n^2 \theta_k h_{n,k}}{\Delta\tau_n} = \frac{\phi_{n+1,k+1/2} - \phi_{n+1,k-1/2}}{\Delta\theta}, \quad (30)$$

where the fluxes in the right-hand side of (30) are approximated by

$$\phi_{n+1,k+1/2} = R_n R_n' \theta_{k+1/2}^2 h_{n+1,k+1/2} + \theta_{k+1/2} h_{n,k+1/2}^a \frac{h_{n+1,k+1} - h_{n+1,k}}{\Delta\theta}, \quad (31)$$

with

$$h_{n,k+1/2} = \frac{h_{n,k+1} + h_{n,k}}{2}. \quad (32)$$

The fluxes at $\theta = 0$ and $\theta = 1$ must obviously be prescribed to be zero, i.e.,

$$\phi_{n+1,1/2} = 0 = \phi_{n+1,K+1/2}. \quad (33)$$

Needless to say that the algorithm above ensures that the volume of the slick remains constant from τ_n to τ_{n+1} .

The numerical scheme (30)–(32) requires the solution of a tridiagonal system of K algebraic equations, which is easily achieved by the relevant version of the LU-decomposition method [9].

In agreement with (15), the time derivative of R is computed by

$$R'_n = \frac{2h_{n,K}^a}{a\Delta\theta R_n}, \quad (34)$$

which allows to advance in time the radius of the slick according to

$$R_{n+1} = R_n + R'_n \Delta\tau_n. \quad (35)$$

After a simple inspection of (17), (18), and (23), one is readily convinced that the characteristic time of the problem under study grows as the radius of the slick increases. Therefore, it is desirable that the time increment $\Delta\tau$ be dynamically adapted as the spreading progresses. In (26), one may identify two different time scales, namely

$$(T_1, T_2) = \left(\frac{R}{R'}, \frac{R^2}{h_{\max}^a} \right), \quad (36)$$

where h_{\max} is the maximum of h taken over the computational domain $0 \leq \theta \leq 1$. To obtain T_1 and T_2 , it was assumed that the time derivative in governing equation (26) was roughly balanced by the first or the second term in the right hand side of (26). The time increment is calculated by

$$\Delta\tau_n = \epsilon \min(T_1(\tau_n), T_2(\tau_n)), \quad (37)$$

where $\epsilon = 0.1$ turned out to be an excellent compromise between numerical accuracy and computer economy. The exact solution indicates that $T_1 < T_2$ if $a < 2$ and that $T_1 \geq T_2$ otherwise. In most cases, the numerical algorithm exhibited a similar behaviour as regards the determination of the time scale.

To assess the quality of the numerical solution, three measures of the error will be used. The first one pertains to the radius of the slick:

$$e_{1,n} = \frac{R_n - R_e(\tau_n)}{R_e(\tau_n)}, \quad (38)$$

where subscript "e" refers to the exact solution. To characterize the shape of the slick, a transformed thickness is defined to be

$$\bar{h} = \frac{\pi a R^2}{(a+1)\Omega} h, \quad (39)$$

which turns out to be an appropriate scaling of h , since, for a constant volume Ω , the order of magnitude of h must decrease as R^2 increases. In particular, when applied to the exact solution, (39) yields $\bar{h}_e(1-\theta^2)^{1/a}$. Relation (39) serves to introduce two error measures that are independent of R and focus on the slick's profile only:

$$e_{2,n}^2 = \frac{\sum_{k=1}^K \theta_k [\bar{h}_{n,k} - \bar{h}_e(\tau_n, \theta_k)]^2}{\sum_{k=1}^K \theta_k [\bar{h}_e(\tau_n, \theta_k)]^2}, \quad (40)$$

and

$$e_{3,n} = \frac{\bar{h}_{n,K} - \bar{h}_e(\tau_n, \theta_K)}{\bar{h}_e(\tau_n, \theta_K)}. \quad (41)$$

The latter error measure pertains to the thickness in the grid box which is closest to the edge.

The time evolution of the radius of the slick is very well reproduced by our numerical method (Figure 4).

It is striking to note that the shape variable \bar{h} and all errors defined above reach, within 5 to 10 time steps, a fairly constant value. This remarkable property, which will be addressed in the next section, may be exploited to greatly simplify the analysis of the results of the numerical simulations. Indeed, one may focus only on the asymptotic limits

$$(e_{i,\infty}, \bar{h}_{\infty,k}) = \lim_{n \rightarrow \infty} (e_{i,n}, \bar{h}_{n,k}), \quad (i = 1, 2, 3). \quad (42)$$

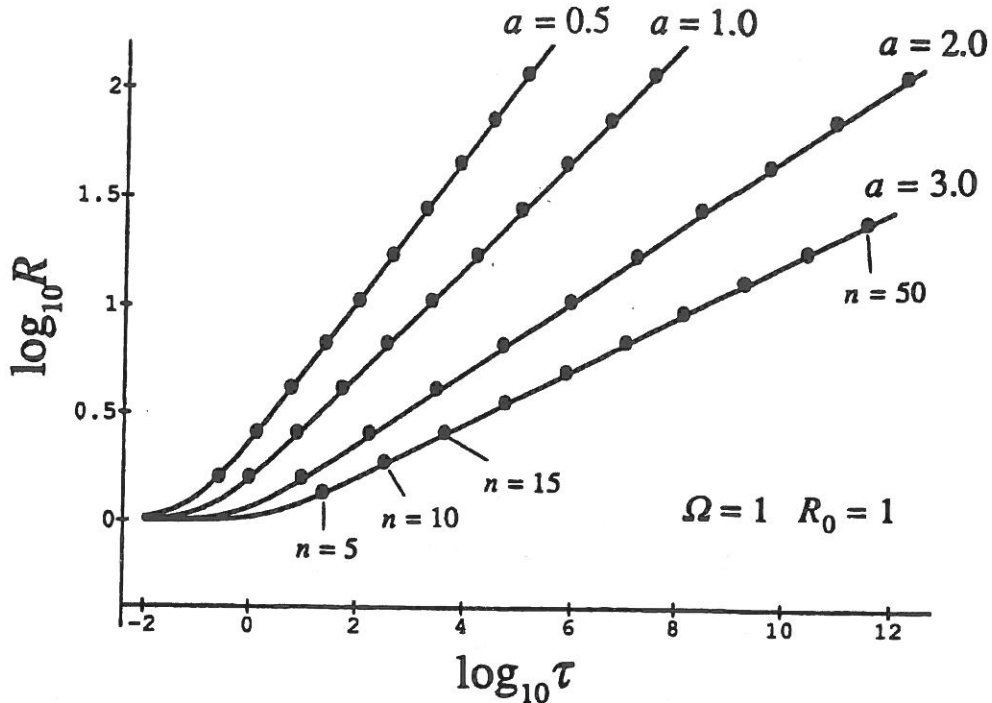


Figure 4. Time evolution of the radius of the slick obtained from the solution of axisymmetric equation (16)—or, equivalently, (26). The curves are from the exact solution (18), in which $\Omega = 1$ and $R_0 = 1$. The dots correspond to the numerical solutions, for which only one value out of five is illustrated ($n = 5, 10, 15, \dots$).

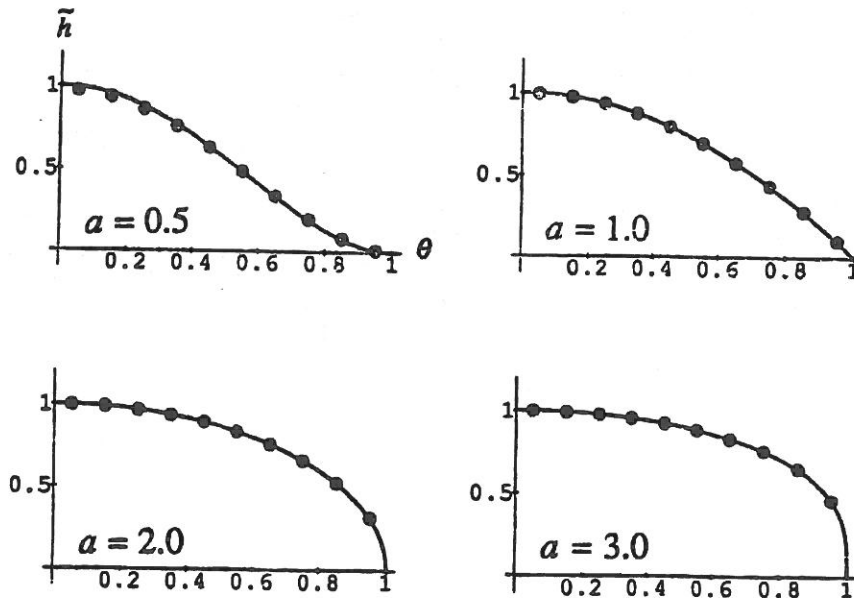


Figure 5. Comparison of the theoretical (curve) and computed (dots) profiles of the slick by means of scaled thickness \tilde{h}_e and $\tilde{h}_{\infty, k}$. The computations were carried out with ten grid points and various values of exponent a .

Figure 5, as well as Tables 1, 2, and 3, clearly point to the high accuracy of the solution procedure used here, even for a coarse discretization encompassing only 5 grid points. All errors are, at most, of the order of a few percent. In accordance with the vast majority of the figures shown in Tables 2 and 3, errors $e_{2, \infty}$ and $|e_{3, \infty}|$ are decreasing functions of K . In other words, increasing the resolution generally leads to an improvement in the representation of the profile of the slick.

Table 1. Relative error in the radius of the slick ($e_{1,\infty}$) in numerical simulations performed with various resolutions—5, 10, and 20 grid points—and different values of a . The appropriate asymptotic form of the edge's velocity is utilized, i.e., relation (34).

$10^2 \times e_{1,\infty}$	$K = 5$	$K = 10$	$K = 20$
$a = 0.5$	1.2	1.9	2.5
$a = 1.0$	3.3	3.7	3.7
$a = 2.0$	3.9	4.2	4.2
$a = 3.0$	2.6	2.9	2.9

Table 2. Relative error in the profile of the slick ($e_{2,\infty}$) in numerical simulations performed with various resolutions—5, 10, and 20 grid points—and different values of a . The appropriate asymptotic form of the edge's velocity is utilized, i.e., relation (34).

$10^2 \times e_{2,\infty}$	$K = 5$	$K = 10$	$K = 20$
$a = 0.5$	2.1	1.8	1.2
$a = 1.0$	0.92	0.24	0.62
$a = 2.0$	0.68	0.23	0.070
$a = 3.0$	0.46	0.18	0.085

Table 3. Relative error in the thickness close to the edge ($e_{3,\infty}$) in numerical simulations performed with various resolutions—5, 10, and 20 grid points—and different values of a . The appropriate asymptotic form of the edge's velocity is utilized, i.e., relation (34).

$10^2 \times e_{3,\infty}$	$K = 5$	$K = 10$	$K = 20$
$a = 0.5$	-1.9	-3.0	-2.3
$a = 1.0$	3.2	2.1	1.1
$a = 2.0$	1.4	0.95	0.55
$a = 3.0$	0.78	0.50	0.27

It may be concluded that our hybrid numerical-asymptotic method is excellent. However, it may also be hypothesized that the high accuracy of the results is partly due to some peculiarities of equation (26) and of its exact solution (17)–(18). In other words, one may imagine that the method examined here is performing extremely well because the case it is applied to turns out to be simplistic. Fully clarifying this issue is beyond the scope of the present study. In the following section, some particular features of our numerical results will be put forward, leaving further investigation of the merit of our hybrid numerical-asymptotic method to a forthcoming paper—in which more general problems will be dealt with.

5. DISCUSSION

The exact solution (17),(18) is such that both the right- and left-hand side of governing equation (26) are zero, i.e.,

$$\frac{\partial}{\partial \tau}(R_e^2 \theta h_e) = 0 \quad (43)$$

and

$$R_e R_e' \theta^2 h_e = -\theta h_e^a \frac{\partial h_e}{\partial \theta}. \quad (44)$$

The numerical solutions exhibit a similar behaviour:

$$R_{n+1}^2 \theta_k h_{n+1,k} \sim R_n^2 \theta_k h_{n,k}, \quad n \rightarrow \infty \quad (45)$$

and

$$R_n R_n' \theta_{k+1/2}^2 h_{n+1,k+1/2} \sim -\theta_{k+1/2} h_{n,k+1/2}^a \frac{h_{n+1,k+1} - h_{n+1,k}}{\Delta \theta}, \quad n \rightarrow \infty \quad (46)$$

Of course, when the initial distribution of h corresponds to h_e , it is easily understood that the adjustment toward (45),(46) may be quick.

We have noticed that, for a wide class of initial profiles of h , convergence toward a regime where (45),(46) hold true also occurs.

Combining (45),(46) with (30)–(33), one gets

$$R'_n \sim \frac{-1}{\Delta\theta \theta_{k+1/2}} \frac{1}{R_n} (h_{n,k+1} - h_{n,k}) h_{n,k+1/2}^{a-1}, \quad n \rightarrow \infty, \quad (47)$$

which is valid for $k = 1, 2, \dots, K-1$. Bearing in mind that R'_n is actually computed by formula (34) in which only $h_{n,K}$ —the thickness in the grid box closest to the edge—appears, one may put forward two opposite interpretations of asymptotic relation (47). Either, it is $h_{n,K}$ that dictates R'_n so that the thickness at all other grid points must adapt in such a way that (47) is verified. Or, it is $h_{n,k}$ that must adapt to the solution inside the slick. One might object that this alternative is formulated in too stark a manner, because it is generally uneasy to clearly identify a cause and its consequences in a nonlinear system. Nonetheless, it turns out that the numerical results are better accounted for by the second proposition.

It follows that the procedure of evaluating the velocity of the edge is eventually not as crucial as initially expected. This may be illustrated as follows.

First, relation (34) is modified to a form that is intentionally made to be incompatible with the outcome of our asymptotic study. For example, we take

$$R'_n = \frac{2h_{n,K}^a}{\Delta\theta R_n}. \quad (48)$$

Notice that (48) is equal to (34) when $a = 1$.

Then, with no other alteration to the numerical scheme, we perform the same simulations as those described previously. As indicated by Table 4, the prediction of the radius of the slick does not become that poorer. Using (48) instead of (34) even improves the accuracy of R_n for $(a, K) = (0.5, 20)$! Thus, the dynamics of h in the interior of the slick forces $h_{n,K}$ to adapt so as to yield a fairly good estimation of the edge velocity, even though formula (48) is not compatible with the spreading regime considered. Not surprisingly, this accommodation is achieved at the expense of the quality of the profile of the slick, which means that errors $e_{2,\infty}$ and $e_{3,\infty}$ are now much higher (Figure 6, Tables 5 and 6).

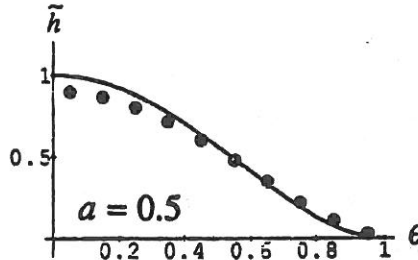


Figure 6. Comparison of the theoretical (curve) and computed (dots) profiles of the slick by means of scaled thickness \tilde{h}_e and $\tilde{h}_{\infty,k}$. The computations were carried out with ten grid points and $a = 0.5$.

Table 4. Relative error in the radius of the slick ($e_{1,\infty}$) in numerical simulations performed with various resolutions—5, 10, and 20 grid points—and different values of a . The intentionally wrong asymptotic form of the edge's velocity is utilized, i.e., relation (48).

$10^2 \times e_{1,\infty}$	$K = 5$	$K = 10$	$K = 20$
$a = 0.5$	-6.5	-2.1	-0.44
$a = 1.0$	3.3	3.7	3.7
$a = 2.0$	8.7	6.7	5.5
$a = 3.0$	8.7	6.0	4.5

Table 5. Relative error in the profile of the slick ($e_{2,\infty}$) in numerical simulations performed with various resolutions—5, 10, and 20 grid points—and different values of a . The intentionally wrong asymptotic form of the edge's velocity is utilized, i.e., relation (48).

$10^2 \times e_{2,\infty}$	$K = 5$	$K = 10$	$K = 20$
$a = 0.5$	15.	8.2	4.5
$a = 1.0$	0.92	0.24	0.062
$a = 2.0$	8.6	5.6	3.2
$a = 3.0$	11.	7.5	4.7

Table 6. Relative error in the thickness close to the edge ($e_{3,\infty}$) in numerical simulations performed with various resolutions—5, 10, and 20 grid points—and different values of a . The intentionally wrong asymptotic form of the edge's velocity is utilized, i.e., relation (48).

$10^2 \times e_{3,\infty}$	$K = 5$	$K = 10$	$K = 20$
$a = 0.5$	240.	200.	250.
$a = 1.0$	3.2	2.1	1.1
$a = 2.0$	-18.	-23.	-26.
$a = 3.0$	-19.	-25.	-28.

The asymptotic relation (45) helps explain why $\tilde{h}_{n,k}$ and $e_{i,n}$ ($i = 2, 3$) reach finite limits as $n \rightarrow \infty$.

From (45), it ensues that $R_n^2 \theta_k h_{n,k}$ does not depend on n in the limit $n \rightarrow \infty$, i.e.,

$$R_n^2 h_{n,k} \sim F_k, \quad n \rightarrow \infty, \quad (49)$$

where F_k is a function of θ_k .

Thus, $\tilde{h}_{\infty,k}$ must depend on θ_k only and must be finite, since the volume of the slick is finite. As a result, $e_{2,n}$ and $e_{3,n}$ tend toward finite limits.

By combining (34), (35), and (48), it may be seen that

$$R_{n+1} \sim R_n + A \frac{\Delta \tau_n}{R_n^{2a+1}}, \quad n \rightarrow \infty, \quad (50)$$

where

$$A = \frac{2F_K^a}{a\Delta\theta}. \quad (51)$$

Assuming that $\Delta \tau_n \ll \tau_n$, (50) implies that

$$R_n \sim B \tau_n^{1/(2a+2)}, \quad n \rightarrow \infty, \quad (52)$$

with

$$B = \left[\frac{4(a+1)}{a\Delta\theta} \right]^{1/(2a+2)} F_K^{a/(2a+2)}. \quad (53)$$

When (28) holds true, the exact analytic expression of the radius (18) admits a simple asymptotic expansion, namely

$$R_e(\tau_n) \sim B_e \tau_n^{1/(2a+2)}, \quad n \rightarrow \infty, \quad (54)$$

with

$$B_e = \left[\frac{4(a+1)^{a+1}}{\pi^a a^{a+1}} \right]^{1/(2a+2)}. \quad (55)$$

Introducing (52) and (54) into (38), in the limit $n \rightarrow \infty$, one has

$$e_{1,\infty} = \frac{B - B_e}{B_e}. \quad (56)$$

One now understands why the relative error on the radius of the slick does tend to a finite limit as n increases.

Of course,

$$\lim_{K \rightarrow \infty} B = B_e. \quad (57)$$

Thus, $|e_{1,\infty}|$ should decrease as the grid size tends to zero. Surprisingly enough, increasing the number of grid points provides poorer predictions of the slick's radius (Table 1). This seemingly counterintuitive phenomenon is partly due to the fact that, with the method used to determine the time step, $\Delta\tau_n$ is not really much smaller than τ_n —which was requested to derive (52)—implying that (52) is not fully valid. Nevertheless, it is worth insisting that the error on the radius, $e_{1,\infty}$, does quickly reach a limit as the resolution increases.

6. CONCLUSION

The asymptotic expression of the edge's velocity (15) leads to excellent numerical results in the single case where we have an exact solution. Whether or not the high accuracy of the results could be retained in more general cases should be examined in another study. However, two different kinds of problems may be anticipated.

First, it is generally necessary to have an exact solution to assess a numerical method. However, obtaining an exact solution for a problem that is less simplistic than that dealt with here will most probably represent a difficult task. Nonetheless, this must be attempted.

Second, it will be necessary to treat problems that are no longer axisymmetric, i.e., fully two-dimensional problems. On a fixed grid (see Appendix), it is likely that the benefit of using the asymptotic evaluation of the edge's velocity will be less significant than with a moving grid fitted to the boundary of the slick. When working out such a solution, potentially intricate mesh generation problems will have to be addressed.

It is now worth recalling that the present study has its roots in some difficulties of Nihoul's model for the transport and spreading of oil slicks on the sea [1–5]. It is doubtless that the results obtained here will help improve the predictions of this model, the applications of which are of high importance in marine pollution problems.

REFERENCES

1. J.C.J. Nihoul, A non-linear mathematical model for the transport and spreading of oil slicks, *Ecol. Modelling* **22**, 325–339 (1984).
2. J.C.J. Nihoul, Modèle de transport et d'étalement des nappes d'hydrocarbures et comparaisons avec les observations, *L'Hydraulique et la Maîtrise du Littoral*, Question No. IV, Rapport No. 10, IV.10.1–IV.10.4, Société Hydrotechnique de France, (1984).
3. J.-M. Brouhon, Modèle d'Evolution d'une Nappe d'Hydrocarbures en Mer—Application au Golfe Persique, Commission des Communautés Européennes, Programme Erasmus, D.E.A. en Modélisation de l'Environnement Marin, Université de Liège, (1992).
4. E. Deleersnijder and A. Loffet, Mathematical modelling and remote sensing of the transport and spreading of spills on the sea, In *Progress in Belgian Oceanographic Research*, (Edited by R. van Grieken and R. Wollast), pp. 92–101, University of Antwerp (UIA), Antwerp, (1985).
5. E. Deleersnijder, Revisiting Nihoul's model for oil slicks transport and spreading on the sea, *Ecol. Modelling* **64**, 71–75 (1992).
6. J. Crank, *The Mathematics of Diffusion*, 2nd edition, Oxford University Press, Oxford, (1975).
7. R. Peyret and T.D. Taylor, *Computational Methods for Fluid Flow*, Springer-Verlag, New York, (1983).
8. J.F. Thompson, Z.U.A. Warsi and C.W. Mastin, *Numerical Grid Generation—Foundations and Applications*, North-Holland, New York, (1985).
9. G. Dahlquist and A. Björck, *Numerical Methods*, Prentice-Hall, Englewood Cliffs, NJ, (1974).

APPENDIX

Here, we describe how the asymptotic expression of the edge's velocity could be used on a fixed two-dimensional Cartesian grid in order to improve the accuracy of an otherwise classical method. It must be realized that the technique suggested below is very crude, but its main advantage is its extreme simplicity.

Consider a grid box of area $\Delta x \times \Delta y$, the center of which is located at $(x_i, y_i) = (i\Delta x, j\Delta y)$ — i and j being integer indices. It is assumed that $h_{n,i,j} \equiv h(t_n, x_i, y_j) > 0$ and that $h_{n,i+1,j} = 0$, i.e., the edge of the slick coincides

with the interface between grid boxes (i, j) and $(i + 1, j)$. At this interface, formula (15) permits evaluating the edge's velocity by

$$u_{x,i+1/2,j} = v_{x,i+1/2,j} + \frac{2h_{n,i,j}^a}{a\Delta x}, \quad (\text{A1})$$

where subscript "x" indicates velocity components along the x-axis. Within one time step Δt , the edge covers the following distance:

$$d_{x,i+1/2,j} = \Delta t u_{x,i+1/2,j}. \quad (\text{A2})$$

If $d_{x,i+1/2,j} < \Delta x/2$, then the interface cannot reach the center of grid box $(i + 1, j)$ before t attains t_{n+1} . In this case, it is proposed to prescribe that the interface between grid box (i, j) and $(i + 1, j)$ is impermeable, implying that no flux, be it advective or diffusive, can cross this interface.

If $d_{x,i+1/2,j} \geq \Delta x/2$, one then allows a flux to go through the interface considered. This flux may be computed by the same discretized forms at those used inside the slick. So doing, $h_{i+1,j}$ will evolve from zero at t_n to a positive value at t_{n+1} .

Of course, operations similar to those described above should be applied to all interfaces of each grid box.

It may be imagined that better results could be obtained by comparing $d_{x,i+1/2,j}$ to a threshold that is slightly different from $\Delta x/2$. Thus, instead of $\Delta x/2$, one might consider $\alpha\Delta x/2$ and perform a series of numerical experiments in order to calibrate α . Obviously, the reasoning put forward in this Appendix would reveal meaningless if it would turn out that the most appropriate value of α is not of order 1.